WWW.IJRPR.COM

International Journal of Research Publication and Reviews

Journal homepage: www.ijrpr.com ISSN 2582-7421

Study Adaptive Backstepping Control for My Quadrotor

Vuong Thuy Linh[1], Chu Manh Tuyen[2], Le Ngoc Giang[3*]

[1]Master, Lecturer, Department of Information Technology, Faculty of General Education, University of Labour and Social Affairs, No. 43, Tran Duy Hung Street, TrungHoa Ward, CauGiay District, Hanoi City, Vietnam

[2]Master, Lecturer, Faculty of Fundamental Technics, AD-AF Academy of Viet Nam, Ha Noi, Vietnam

[3]PhD, Head of Metrology Department, Faculty of Fundamental Technical, AD-AF Academy of Vietnam

DOI: https://doi.org/10.55248/gengpi.2023.32716

A B S T R A C T

Controlling the flight of a quadrotor is a challenging task due to the complexity of the flight trajectory program and the uncertain changes in aerodynamic parameters. These factors contribute to the system's nonlinear and complicated nature. Flight path angle tracking control involves various channels, such as a pitch controller, a roll controller, and a yaw controller. Traditionally, these channels are designed using linear control methods, which may not always be satisfactory. A more effective approach to controller design is the use of backstepping. Backstepping control laws not only provide certain gain margins for the controllers but also handle model errors in the description of aerodynamics.

This paper proposes a backstepping nonlinear controller design method for quadrotor control systems. Simulation results demonstrate that the control strategy presented in this paper is effective and has strong robustness in the presence of disturbances and parameter uncertainty. The proposed approach addresses the challenges associated with traditional linear control methods and offers a more efficient and robust solution to quadrotor flight control.

Keywords: Quadrotor, Backstepping, nonlinear controller

1. Introduction

A quadrotor is an unmanned aerial vehicle that utilizes vertical take-off and landing. It consists of two pairs of propellers arranged symmetrically, with each pair rotating in opposite directions as illustrated in Figure 1. The quadrotor's structural components include mechanical, transmission, automatic control, sensing, receiving, and transmitting information systems.

The quadrotor is a control object with a dynamic model represented by nonlinear equations containing uncertain parameter components. The motion of the quadrotor can be divided into various channels such as tilt, flip, rotation, angular velocity, and angular acceleration in the three XYZ axes.

The backstepping control method is a recently developed nonlinear design method that can selectively handle nonlinear factors [1]. Adaptive backstepping control can provide convergence assessment for unknown parameters [4]. In this article, the authors conduct research on designing adaptive backstepping and backstepping controllers for quadrotors to enhance control quality, expand the working range, and increase adaptability in the presence of uncertain factors. The proposed approach offers a promising solution for improving the performance of quadrotor systems.

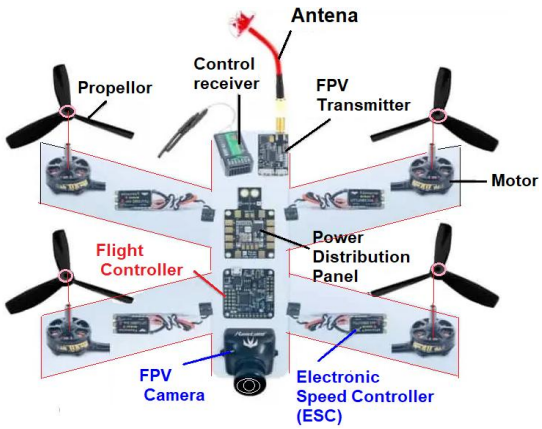

Fig.1. Basic structure of a quadrotor

2. Building a mathematical model for my quadrotor

The control object can be viewed as being split into two systems that work in conjunction with each other. The first system is the engine model of the propeller described by the system of equations (1), and the second system is the propeller dynamics system described by the system of equations (2.a). These two systems are related to each other through the relationship between the rotational speed Ω $(\omega_1, \omega_2, \omega_3, \omega_4)$ of the four motors, the lifting force Fz, and the torque (T_x , T_y , T_z).

2.1. A mathematical model of the propeller engine

The most common type of motor currently applied to quadrotors is the BLDC motor. According to [4], the system of equations describing the mathematical model of a DC motor has the following form:

$$\begin{cases} j\omega = K_t.I_a - b.\omega - T_{load} \\ V_a = R_a.I_a + L_a.\frac{dI_a}{dt} + K_b.\omega \end{cases} \quad (1)$$

The first equation describes the relationship between the force moment and the electromagnetic moment. The second equation describes the relationship between the voltage applied to the motor and the current; j is the moment of inertia of the propeller motor; $\dot{\omega}$ is the angular acceleration of the motor; Ia is the supply current; b is the drag torque coefficient; Kt is the motor torque coefficient; Tload is the load torque; Va is the supply voltage; Ra is the impedance of the motor; La is the motor inductance; and Kb is the reactance coefficient.

2.2. The dynamic model of the Quadrotor

To establish a mathematical model for the quadrotor, we need to consider some related coordinate systems, as shown in Figure 2. In which, Oxyz is the inertial coordinate system and Bxyz is the associative coordinate system, which is closely tied to the fixed frame of the quadrotor. Call the quadrotor's three Euler rotations around the three axes, respectively, as shown in Figure 2, the tilt angle Φ, the pitch angle θ and the direction angle Ψ. And F_1, F_2, F_3, F_4 are the thrust caused by the four propellers, respectively.

To analyze the dynamics of the quadrotor, we consider it an absolutely rigid body moving freely through space. From there, we divide the motion of the quadrotor into two components: the translational motion of the center of mass and the rotation motion of the quadrotor about its three axes. The translational motion is caused by the drag and lift force components, while the rotational motion is caused by the force moments.

For convenience and simplicity when considering the dynamic properties of the quadrotor, we do not consider the part of the DC motor that rotates the propeller, and the control signal of the system is converted to the force as well as the torque to be generated. Therefore, the principle of controlling the quadrotor is as follows: The motion of the quadrotor is controlled through four components: the total force F along the axis Bz; the torque Tx on the axis Bx; the torque Ty on the By axis; and the torque Tz on the axis Bz; and $-F_L=U_1$. It is the F component that makes the quadrotor changeable in height, the Tx and Ty components that cause edge motion along the Bx and By axes, and the Tz component that helps to change the direction around the Bz axis.

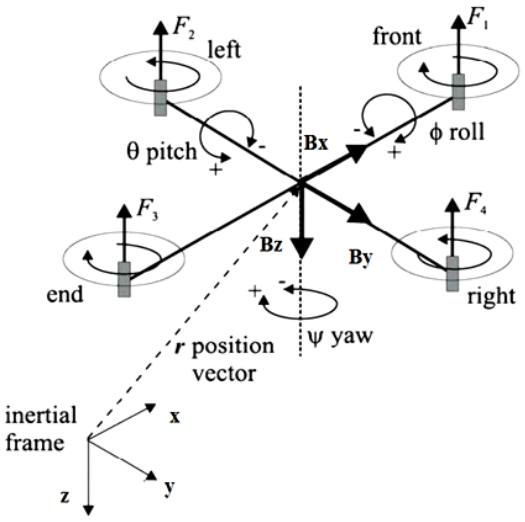

Fig.2. Coordinate systems of the quadrotor

It is assumed that the Euler rotations are small and have little effect on the rotation of the quadrotor, while ignoring the effect of the gyro effect on the quadrotor caused by the four propeller motors. We get the complete system of nonlinear kinematic equations for the quadrotor:

$$\begin{cases} \ddot{\Phi} = \dot{\Psi}.\dot{\theta}.\dfrac{J_{yy} - J_{zz}}{J_{xx}} + \dfrac{T_x}{J_{xx}} \\ \ddot{\theta} = \dot{\Psi}.\dot{\Phi}\dfrac{J_{zz} - J_{xx}}{J_{yy}} + \dfrac{T_y}{J_{yy}} \\ \ddot{\Psi} = \dfrac{T_z}{J_{zz}} \\ \ddot{x} = \left(cos\Phi.sin\theta.cos\Psi + sin\Phi.sin\Psi\right).\dfrac{1}{m}.\left(-F_L\right) \\ \ddot{y} = \left(cos\Phi.sin\theta.sin\Psi - sin\Phi.cos\Psi\right).\dfrac{1}{m}.\left(-F_L\right) \\ \ddot{z} = g + cos\Phi.cos\theta.\dfrac{1}{m}.\left(-F_L\right) \end{cases} \quad (2a)$$

2.3. A quadrotor dynamics model, taking into account uncertainties

The system of equations (2.a) is the result of calculation after applying a few assumptions to simplify, such as: consider the tilt angle Φ and the slope angle θ as two small motion angles, eliminating the influence of gyro torque on channel Φ. In fact, the mathematical model is much more complex with the cross-relationship between the channels Φ, θ and Ψ. There is also an additional gyro-torque component. Therefore, the actual mathematical model of the object will contain uncertain components:

$$\begin{cases} \ddot{\Phi} = \dot{\Psi}.\dot{\theta}.\dfrac{J_{yy} - J_{zz}}{J_{xx}} + \dfrac{T_x}{J_{xx}} + f_1.\dot{\theta} + f_2.\theta + f \\ \ddot{\theta} = \dot{\Psi}.\dot{\Phi}.\dfrac{J_{zz} - J_{xx}}{J_{yy}} + \dfrac{T_y}{J_{yy}} + f_3.\dot{\Phi} + f_4.\Phi + f \\ \ddot{x} = \left(cos\Phi.sin\theta.cos\Psi + sin\Phi.sin\Psi\right).\dfrac{1}{m}.\left(-F_L\right) - f_x.\dot{x} \\ \ddot{y} = \left(cos\Phi.sin\theta.sin\Psi - sin\Phi.cos\Psi\right).\dfrac{1}{m}.\left(-F_L\right) - f_y.\dot{y} \\ \ddot{z} = g + cos\Phi.cos\theta.\dfrac{1}{m}.\left(-F_L\right) + f_z \end{cases} \quad (2b)$$

3. Designing a controller for my quadrotor

Below, the author synthesizes adaptive backstepping and backstepping controllers as follows:

The main content of the synthesis of the backstepping controller is to give the control law for each control channel, provided that the parameters in the kinematic model of the quadrotor are clear. Below are the steps to synthesize the backstepping controller according to the z-height channel. The synthesis of the backstepping controller for x and y channels and according to tilt angle Φ, direction angle Ψ, pitch angle θ is completely similar.

For the z channel, we have a system of kinematic equations:

$$\ddot{z} = g + cos\Phi.cos\theta.\frac{1}{m}.(-F_L)$$

Set $X_1 = z$; $X_2 = \dot{z}$; and $F_L = U_1$, so $X_1 = \dot{z}$ and $X_2 = \ddot{z}$. From this, the model of tight backpropagation along the z-channel is:

$$\begin{cases} \dot{X}_1 = X_2 \\ \dot{X}_2 = g + cos\Phi.cos\theta.\frac{1}{m}.(-U_1) \end{cases} \quad (3)$$

Call the desired altitude signal zd, and $X_1 = z$.

Step 1: Set $Z_1 = X_1 - z_d$.

So $Z_1 = X_1 - z_d = X_2 - z_d$.

Select the control function Lyapunov $V_1(Z_1) = \frac{1}{2}Z_1^2$; the condition for signal $X_1 \to z_d$ is:

$$\dot{V}_1(Z_1) = Z_1.\dot{Z}_1 = .Z_1.(X_2 - \dot{z_d}) < 0 \quad \forall Z_1 \neq 0$$

Considering x2 is a virtual control signal, deducing the virtual control law to ensure the stability criterion of Lyapunov is: $X_{2d} = -C_1.Z_1 + z_d$ with C1 > 0.

Step 2: Set $Z_2 = X_2 - z_{2d}$. So

$$Z_2 = X_2 - X_{2d} = g + cos\Phi.cos\theta.\frac{1}{m}.(-U_1) + C_1.Z_1 - z_d$$

Inferred $V_1(Z_1) = Z_1.(-C_1.Z_1 + Z_2)$

Select the control function Lyapunov $V_2(Z_1, Z_2) = V_1 + \frac{1}{2}Z_2^2$; the condition for signal $X_2 \to X_{2d}$ is:

$$\dot{V}_2 = \dot{V}_1 + Z_2.\dot{Z}_2 < 0 \quad \forall\ Z_1, Z_2 \neq 0$$

$$V_2 = -C_1.Z_1^2 + Z_1.Z_2 + Z_2.\left(g + cos\Phi.cos\theta.\frac{1}{m}.(-U_1) + C_1.Z_1 - z_d\right)$$

From the Lyapunov stability criterion, to ensure the system is globally asymptotically stable, the control law U1 has the following form:

$$U_1 = m\frac{1}{cos\Phi.cos\theta}\left(Z_1 + g + C_1.Z_1 - z_d + C_2.Z_2\right)$$

Ignoring the higher-order derivatives, we get that the control law for the z channel is:

$$(\quad)U_z = m\frac{1}{cos\Phi.cos\theta}Z_1 + g + C_2.Z_{\quad 2} + C_1.Z_2 - C_1^2.Z_1$$

Similarly, we have the control law for the channels x, y, and Φ, θ, Ψ as:

$$U_x = m\frac{1}{U_z}(Z_3 + C_4.Z_4 + C_3.Z_4 - C_3^2.Z_3)$$

$$U_y = m\frac{1}{U_z}(Z_5 + C_6.Z_6 + C_5.Z_6 - C_5^2.Z_5)$$

$$U_\Phi = J_{xx}.\left(-Z_7 - \Psi.\theta.\frac{J_{yy} - J_{zz}}{J_{xx}} - C_8.Z_8 - C_7.Z_8 + C_7^2.Z_7\right)$$

$$U_\theta = J_{yy}.\left(-Z_9 - \Psi.\Phi.\frac{J_{zz} - J_{xx}}{J_{yy}} - C_{10}.Z_{10} - C_9.Z_{10} + C_9^2.Z_9\right)$$

$$U_\Psi = J_{zz}.(-Z_{11} - C_{12}.Z_{12} - C_{11}.Z_{12} + C_{11}^2.Z_{11})$$

where C_i are positive design constants.

4. Backstepping controller design for propeller motor

As analyzed, the control of the quadrotor must be through the actuators, which are DC motors with propellers. The control quality of the quadrotor is directly affected by the control quality of these four motors. As with these motors, the faster the response, the better the maneuverability of the quadrotor, and vice versa.

The dynamic model of the motor used in this study is an independently excited DC motor. The author also applies the backstepping control algorithm to stabilize the motor's rotation speed in accordance with the required load torque.

The system of dynamic equations for a DC motor, according to (1), is:

$$\begin{cases} j\omega = K_t.I_a - b.\omega - T_{load} \\ V_a = R_a.I_a + L_a.\dfrac{dI_a}{dt} + K_b.\omega \end{cases}$$

Putting X1=ω, X2=Ia, U=Va, converting the above system to tight backpropagation, we get:

$$\begin{cases} X_1 = -\dfrac{b}{j}.X_1 - \dfrac{K_M}{j}.X_1^2 + \dfrac{K_t}{j}.X_2 \\ X_2 = -\dfrac{K_b}{L_a}.X_1 - \dfrac{R_a}{L_a}.X_2 + \dfrac{1}{L_a}U \end{cases}$$

Let the desired rotational speed of the motor be ωd. Set Z1=X1-ωd, when the rotation speed signal ω→ωd, then Z1→0. On the other hand, with $\dot{X}_1 = \dot{Z}_1 + \dot{\omega}_d$, substituting into the first equation of the system, we have:

$$Z_1 = -\frac{b}{j}.X_1 - \frac{K_M}{j}.X_1^2 + \frac{K_t}{j}.X_2 - \omega_d$$

Similar to applying the backstepping algorithm to the state channels discussed above, we need a virtual control signal, X2→X2d. Finally, according to the Lyapunov asymptotic stability criterion, for the system to be globally stable, the necessary control signal U has the following form:

$$U = L_a.\left[-\frac{K_t}{j}.Z_1 - f_2(Z_1, Z_2) - C_2.Z_2\right]$$

In which: $C_1, C_2 > 0$

$$f_2(Z_1, Z_2) = -\left[\frac{b}{K_t} + \frac{K_M}{K_t}.2.X_1 - \frac{j}{K_t}C_1\right].\left[-C_1.Z_1 + \frac{K_t}{j}.Z_2\right] - \frac{K_b}{L_a}X_1 - \frac{R_a}{L_a}.X_2$$

Each motor should have a rotary speed stabilizer, as shown above.

5. Adaptive Backstepping Controller Design for Quadrotor

5.1. Consider the Φ-angle channel

The mathematical model of the channel Φ when considering the uncertainty components in the tight backpropagation form is as follows:

$$\begin{cases} X_7 = X_8 \\ X_8 = \Psi.\theta.\dfrac{J_{yy} - J_{zz}}{J_{xx}} + f_1.\theta + f_2.\theta + f + \dfrac{U_2}{J_{xx}} \end{cases}$$

Let the desired tilt angle signal Φ be Φd.

Set $Z_7=X_7-\Phi_d$, if $X_7 \rightarrow \Phi_d$ then $Z_7 \rightarrow 0$.

Set $Z_8=X_4-X_{8d}$, if $X_8 \rightarrow X_{8d}$ then $Z_8 \rightarrow 0$.

Transforming the above system in terms of Z_7 and Z_8, we get:

$$\begin{cases} Z_7 = X_8 - \Phi_d \\ Z_8 = \Psi.\theta.\dfrac{J_{yy} - J_{zz}}{J_{xx}} + f_1.\theta + f_2.\theta + f + \dfrac{U_2}{J_{xx}} - X_{8d} \end{cases}$$

From the results of the synthesis of the backstepping control law for channel Φ, done in the previous section, the adaptive control law has the form:

$$U_\Phi = J_{xx}.\left(-Z_7 - \Psi.\theta.\frac{J_{yy} - J_{zz}}{J_{xx}} - C_7.Z_8 + C_7^2.Z_7 - C_8.Z_8 - \hat{f}_1.\theta - \hat{f}_2.\theta - \hat{f}\right)$$

where $\hat{f}_1$ and $\hat{f}_2$ are estimates of the uncertainty component.

Let the estimated errors of f_1, f_2, and f_3 be: $\tilde{f}_1 = f_1 - \hat{f}_1; \tilde{f}_2 = f_2 - \hat{f}_2; \tilde{f} = f - \hat{f}$

Putting the estimated error components into the Lyapunov control function component:

$$V_8\left(Z_7, Z_8, \tilde{f}_1, \tilde{f}_2.\tilde{f}\right) = V_8(Z_7, Z_8) + \frac{1}{2.\gamma_1}.\tilde{f}_1^2 + \frac{1}{2.\gamma_2}.\tilde{f}_2^2 + \frac{1}{2.\gamma}.\tilde{f}^2$$

where $\gamma_1,\ \gamma_2, \gamma$ are the adaptation coefficients. If we differentiate with respect to time, we get:

$$V_8 = -C_7Z_7^2 + Z_8.\left[Z_7 + \Psi.\theta.\frac{J_{yy} - J_{zz}}{J_{xx}} + f_1.\theta + f_2.\theta + f + \frac{U_2}{J_{xx}} + C_7.Z_7\right] + \frac{1}{\gamma_1}.\tilde{f}_1.\dot{\tilde{f}}_1 + \frac{1}{\gamma_2}.\tilde{f}_2.\dot{\tilde{f}}_2 + \frac{1}{\gamma}.\tilde{f}.\dot{\tilde{f}}$$

Substituting U_Φ, get:

$$V_8 = -C_7Z_7^2 + Z_8.\left[-C_8.Z_8 + \tilde{f}_1.\theta + \tilde{f}_2.\theta + \tilde{f}\right] + \frac{1}{\gamma_1}.\tilde{f}_1.\dot{\tilde{f}}_1 + \frac{1}{\gamma_2}.\tilde{f}_2.\dot{\tilde{f}}_2 + \frac{1}{\gamma}.\tilde{f}.\dot{\tilde{f}}$$

Using the same reasoning as in the non-adaptive case, in order to ensure that the system is globally asymptotically stable according to the Lyapunov criterion, deduce the correction rule for the estimation of the uncertain parameters:

$$\begin{cases} \frac{1}{\gamma_1}.\dot{\tilde{f}}_1 + Z_8.\theta = 0 \\ \frac{1}{\gamma_2}.\dot{\tilde{f}}_2 + Z_8.\theta = 0 \\ \frac{1}{\gamma}.\dot{\tilde{f}} + Z_8 = 0 \end{cases} \Rightarrow \quad \begin{cases} \dot{\tilde{f}}_1 = -Z_8.\theta.\gamma_1 \\ \dot{\tilde{f}}_2 = -Z_8.\theta.\gamma_2 \\ \dot{\tilde{f}} = -Z_8.\gamma \end{cases} \Rightarrow \begin{cases} \hat{f}_1 = Z_8.\theta.\gamma_1 \\ \hat{f}_2 = Z_8.\theta.\gamma_2 \\ \hat{f} = Z_8.\gamma \end{cases}$$

5.2. Considering the θ-angle channel

The same reasoning as above, we have the adaptive backstepping control law for channel θ as follows:

$$U_{\boldsymbol{\theta}} = J_{yy}.(-Z_9 - \Psi.\Phi.\frac{J_{zz} - J_{xx}}{J_{yy}} - C_{10}.Z_{10} - C_9.Z_{10} + C_9^2.Z_9 - \hat{f}_3.\Phi - \hat{f}_4.\Phi - \hat{f})$$

The correction law is defined as follows:

$$\begin{cases} \hat{f}_3 = Z_{10}.\Phi.\gamma_3 \\ \hat{f}_4 = Z_{10}.\Phi.\gamma_4 \\ \hat{f} = Z_{10}.\gamma \end{cases}$$

Where γ_3, γ_4, γ are the adaptation coefficients.

5.3. Consider the channels x, y, and z

The same reasoning as above, we have adaptive backstepping control laws for x, y, and z channels as follows:

$$U_x = m\frac{1}{U_1}\left(Z_3 + C_4.Z_4 + C_3.Z_4 - C_3^2.Z_3 - \hat{f}_x.(-C_3.Z_3 + Z_4)\right)$$

$$U_y = m\frac{1}{U_1}\left(Z_5 + C_6.Z_6 + C_5.Z_6 - C_5^2.Z_5 - \hat{f}_y.(-C_5.Z_5 + Z_6)\right)$$

$$U_z = m\frac{1}{cos\Phi.cos\theta}\left(Z_1 + g + C_2.Z_2 + C_1.Z_2 - C_1^2.Z_1 + \hat{f}_z\right)$$

The correction law is defined as follows:

$$\hat{f}_x = (-Z_4^2 + C_3.Z_3.Z_4).\gamma_x;$$

$$\hat{f}_y = (-Z_6^2 + C_5.Z_5.Z_6).\gamma_y;$$

$$\hat{f}_z = Z_2.\gamma_z$$

Where $\gamma_x;\gamma_y;\gamma_z$ are the adaptation coefficients.

6. Simulation results

The parameters of the motor and the initial parameters are selected as follows:

j=6.10^(-5) kg.m2; b=3,36.10^(-5)kg.m2/s; Kt=0,0052; Ra=0,9Ω; La=2mH; b=0,0057; Km=7,5.10^(-7); Kf=3,13.10^(-5); m=0,65kg; g=9,81m/s2; ixx=7,5.10^(-3) kg.m2; iyy=7,5.10^(-3)kg.m2; izz=1,3.10^(-2) kg.m2; L=0,23m; u10=m.g N;

6.1. Backstepping controller review

The backstepping control diagram is as follows:

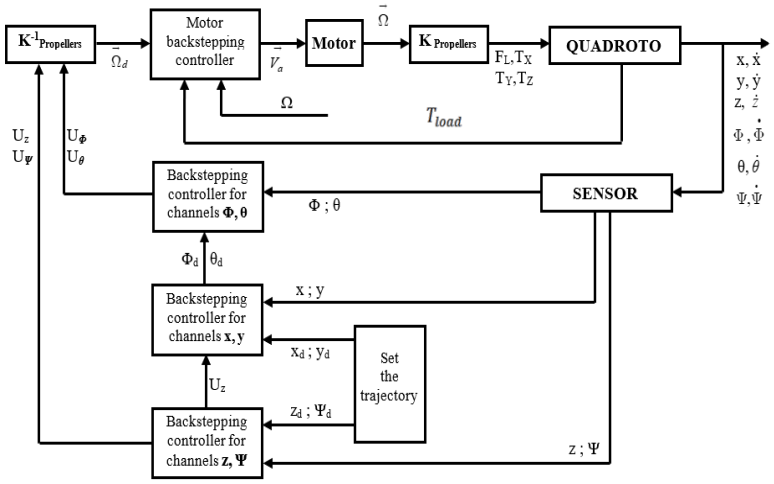

Fig.3. Backstepping control diagram for quadrotor

Consider the stable mode of all 3 parameters x, y, and z of the quadrotor at the same time to evaluate the control quality of backstepping when there is a phenomenon of crossover channels.

The wanted input signals (xd, yd, and zd) all have the form of a step function, which is fed into the system at the same time. Through simulation and comparison, it can be concluded that the control quality of the backstepping orbital stabilizer is superior to that of the PID orbital stabilizer, which is shown by:

- First, the control quality in the backstepping transition is better than that of the PID, as demonstrated by the shorter transient time, less oscillation, and smaller overshoot.

- Second, the working band on the backstepping channels is wider than that of the PID, which increases the quadrotor's mobility in trajectory control and tracking, and at the same time helps the quadrotor not to be unstable when encountering large disturbances causing changes. sudden change in the kinematic parameters of the quadrotor.

- Third, backstepping still ensures control quality in cases of crossover channels.

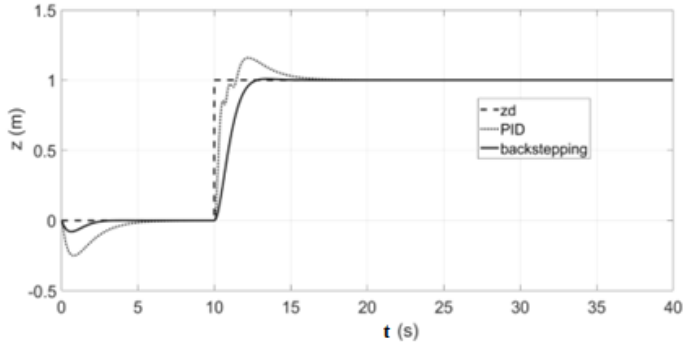

Fig.4. Control results on channel Z

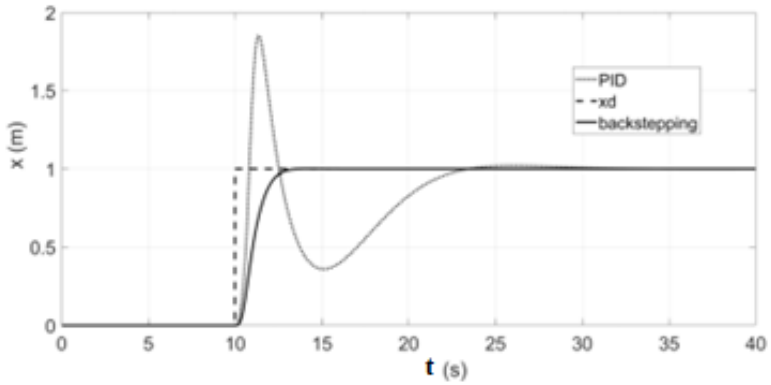

Fig.5. Control results on channel X

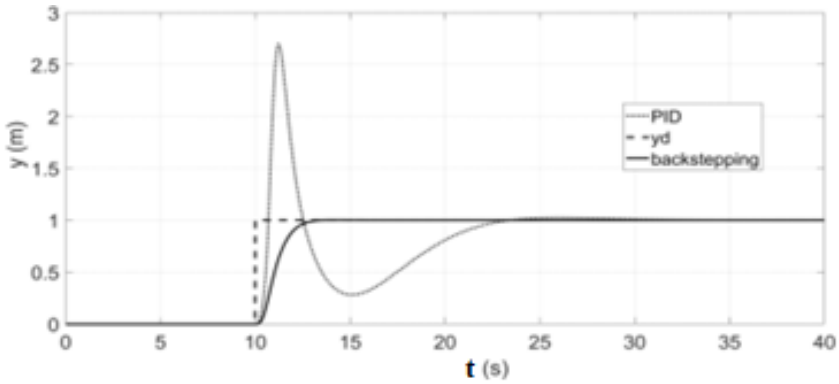

Fig.6. Control results on channel Y

6.2. Adaptive backstepping controller evaluation

In the above, a mathematical model of a quadrotor has been given with possible uncertain components due to the existence of an uncertain dynamic component, changes in the weight of the quadrotor, noise, or drag... Below, the author analyzes the effect of an adaptive backstepping orbital stabilizer on control quality on channels θ and X when there is noise on channel θ. The angle channel Φ, y channel, and z channel can be done similarly.

The mathematical model of channel θ taking into account the uncertainty component has the following form:

$$\theta = \Psi.\Phi.\frac{J_{zz} - J_{xx}}{J_{yy}} + \frac{T_y}{J_{yy}} + f_3.\Phi + f_4.\Phi + f$$

The adaptive backstepping control scheme for the Picht channel θ is depicted in Figure 7 below.

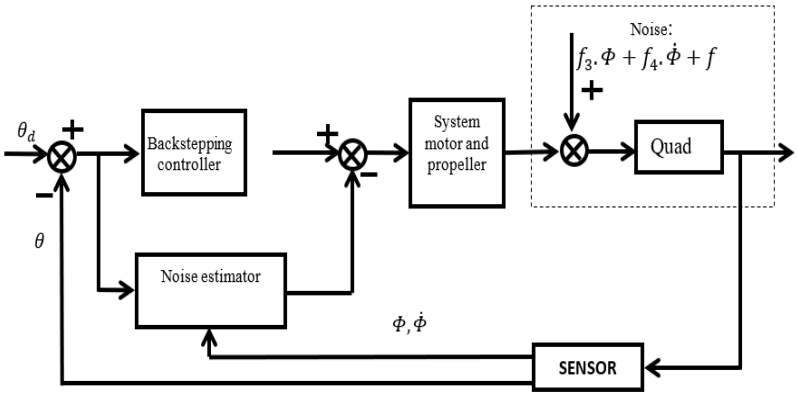

Fig.7. Adaptive backstepping control diagram for the θ-channel

To evaluate the control quality of the system when applying adaptive backstepping, the author conducts a survey in the following cases:

- *Case 1:* Consider the impact noise as an uncertain component f on channel θ with pulse shape as shown in Figure 8. The input signal of channel θ is θd in the form of a step function.

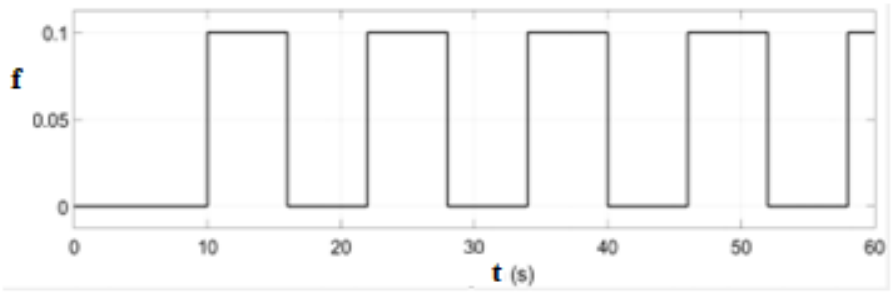

Fig.8. Noise in the form of pulses

Figure 9 depicts the control results on θ-channel when available uncertainty noise in the form of pulses.

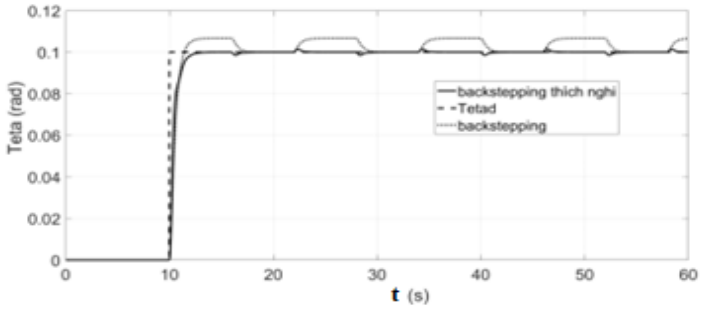

Fig.9. The control results on θ-channel when available uncertainty noise in the form of pulses

- *Case 2:* Consider the impact noise as an uncertain component f on channel θ with the form of a sine function, with the value shown in Figure 10. The input signal of channel θ is θd in the form of a step function.

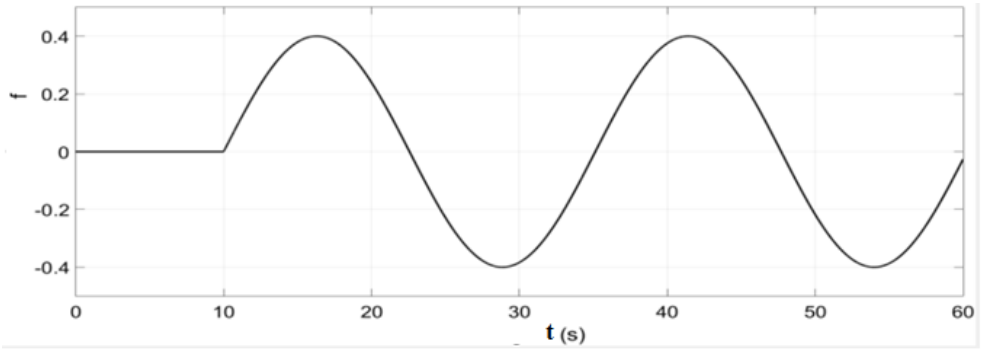

Fig.10. Sinusoidal noise

Figure 11 depicts the control results on θ-channel when available uncertainty noise in the form of Sinusoidal.

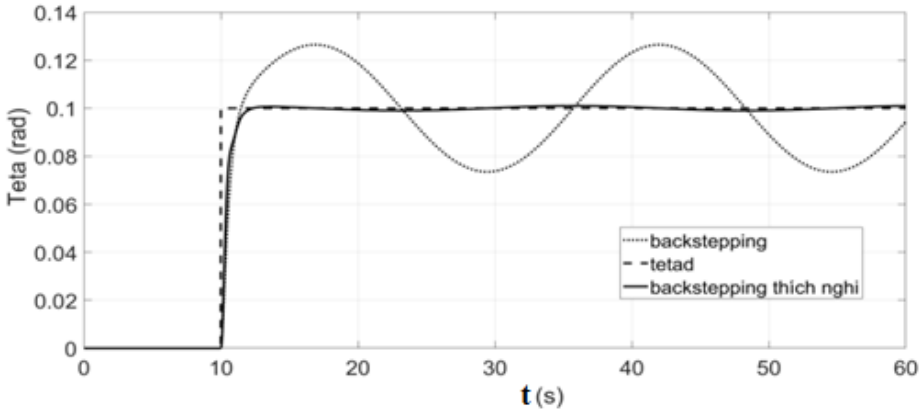

Fig.11. The control results on θ-channel when available uncertainty noise in the form of Sinusoidal

- Case 3: Consider the impact noise as the uncertainty component caused by the gyro torque $-J_r.\Phi.\Omega_r/J_{yy}$ acting on channel θ. The author investigates the adaptive backstepping controller in the following modes: On the 0y axis, the control quadrotor oscillates around the equilibrium point y0=0. The input signal yd is pulsed. On the 0x axis, the quadrotor control stabilizes at x0=0.

Theoretically, when there is movement on the 0y axis, there will be a change in rotation angle Φ and rotation angle speed $\dot{\Phi}$. On the other hand, the angular momentum of the propeller system occurs due to the difference in rotational speeds of the two pairs of propellers that are always rotating in opposite directions. The angular momentum of the propeller system is calculated as follows: $\vec{H} = J_r.\overrightarrow{\Omega_r}$

The angular momentum combined with the variation of the tilt angle Φ gives rise to a gyro moment affecting the channel θ. The gyro moment is calculated as follows:

$$\vec{M}_{gi} = \vec{H}.\vec{\Phi}$$

Notice that the $\overrightarrow{M_{gi}}$ vector has a similar form to the considered uncertainty component $f_3.\dot{\Phi}$. This uncertainty component acts on the channel θ, leading to a change in θ and a variation of x around the equilibrium position x0.

Figure 12 depicts the variation of the gyro torque acting on the channel θ.

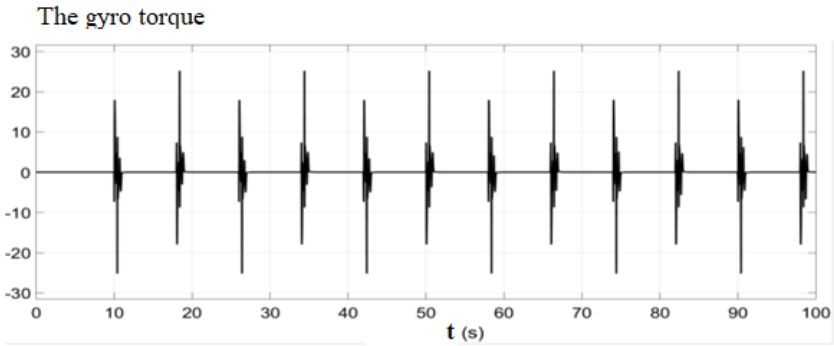

Fig.12. The gyro torque acting on the channel θ

Figure 13 depicts the variation of the angle θ due to the influence of the gyroscope torque.

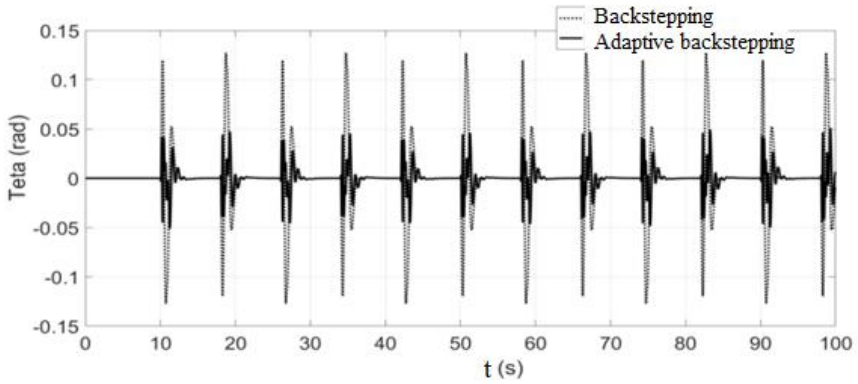

Fig.13. The variation of the angle θ due to the influence of the gyroscope torque

Due to the variation of the pitch angle θ, the quadrotor oscillates around the equilibrium position x0 on the 0x axis, as depicted in Figure 14.

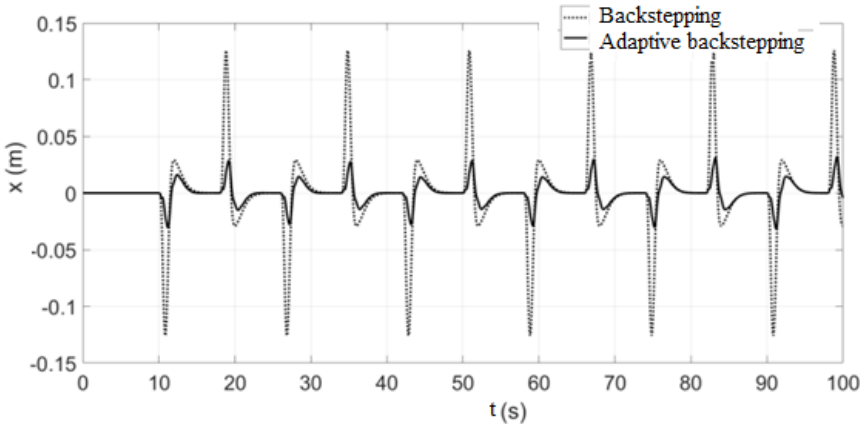

Fig.14. Variation of x due to influence of gyro torque

From the results in Figures 13 and 14, it is shown that in the orbital stabilization mode at x0=0, when affected by the gyro torque, the adaptive backstepping controller gives better results than the backstepping controller. This is shown by the fact that the amplitude of oscillation on the x channel is significantly reduced.

4. Conclusion

In this study, the authors have made a new contribution by dividing the mathematical modeling of the quadrotor system into two systems that are bound together, resulting in a closer representation of reality. The first system is characterized by a nonlinear mathematical model describing quadrotor kinematics, while the second system is characterized by a mathematical model of a DC motor and the relationship between propeller thrust and rotational speed. This is an important mathematical basis that ensures the synthesis of quality adaptive backstepping and backstepping controllers.

The simulation results have shown the outstanding advantages of the backstepping controller compared to the PID controller, namely the fast setting time and maneuverability of the quadrotor at a larger working range. Additionally, the application of an adaptive backstepping controller to stabilize the trajectory produces better results than a conventional backstepping controller. It helps to suppress the influence of uncertain components and reduce the impact of noise during quadrotor operation.

When dealing with strong nonlinear systems such as quadrotors, the control law is usually designed using the adaptive backstepping method, which is capable of compensating for uncertainties in the model and improving the stability of the control system. However, one limitation of the adaptive backstepping method is that the calculation of the virtual control law can be very complex, and control law synthesis is only possible under suitable conditions. On the other hand, the sliding controller is invariant and stable to internal uncertainties and external disturbances. Therefore, combining the sliding control mode with the backstepping technique can provide an effective solution for developing a robust controller for strict-feedback nonlinear systems with a simple design procedure that takes advantage of the benefits of both methods. This is an area of focus for the authors' future research.

ACKNOWLEDGEMENT

This work is supported by: Department of Information Technology, Faculty of General Education, University of Labour and Social Affairs in Hanoi Vietnam. Faculty of Fundamental Technics, AD-AF Academy of Viet Nam.

REFERENCES

Lê Ngọc Giang, Mai Khánh Dương, Nguyễn Đức Việt. *Điều khiển quỹ đạo máy bay Su-22 sử dụng phương pháp thiết kế cuốn chiếu*. VCCA-2017. pp. 107-117, ISBN 978-604-73-5569-3, 12/2017.

Duc, T.N., Ngoc, T.N., Le Ngoc, G., Xuan, T.T.. *Determining for Launcher Distance and Intersection Point of Missile and Target Using Simulation Method*. Lecture Notes in Networks and Systemsthis link is disabled, 2021, 243, pp.181–188.

Giang, L.N., Kaipei, L. *Simple backstepping control design for the rotor - Side converter of a DFIG wind turbine generator*. International Journal of Applied Mathematics and Statistics, 2013, 51(21), pp. 396–405.

Robert Mahony, Vijay Kumar. Modelling, *Estimation and Control of Quadrotor Aerial Vehicles*. Robotics and Automation Magazine. 2012.

H. Bouadi, M. Bouchoucha and M.Tadjine. *Modelling and Stabilizing Control Laws Design Based on Sliding Mode for an UAV Type – Quadrotor*. Engineering Letters. 2007.

M. Hassanalian, A. Abdelkefi. *Classifications, applications, and design challenges of drones: a review*. Progress in Aerospace Sciences. vol. 91, pp. 99–131, 2017.

H. Mo and G. Farid. *Nonlinear and adaptive intelligent control techniques for quadrotor uav - a survey*. Asian Journal of Control. Vol. 21, no. 2, pp. 989–1008, 2019.

Y. Zhong, Y. Zhang, W. Zhang, J. Zuo, H. Zhan. *Robust actuator fault detection and diagnosis for a quadrotor UAV with external disturbances*. IEEE Access. Vol. 6, 2018.

Y. Zhang, Z. Chen, X. Zhang, Q. Sun, M. Sun. *A novel control scheme for quadrotor UAV based upon active disturbance rejection control*. Aerospace Science and Technology. Vol. 79, pp. 601–609, 2018.

B. C. Zheng, X. Yu, and Y. Xue. *Quantized sliding mode control in delta operator framework. International Journal of Robust and Nonlinear Control*. Vol. 28, no. 2, pp. 519–535, 2018.

X. Zhang. *Robust integral sliding mode control for uncertain switched systems under arbitrary switching rules*. Nonlinear Analysis: Hybrid Systems. Vol. 37, Article ID 100900, 2020.

S. Liu, Y. Liu, N. Wang. *Nonlinear disturbance observer-based backstepping finite-time sliding mode tracking control of underwater vehicles with system uncertainties and external disturbances*. Nonlinear Dynamics. Vol. 88, no. 1, pp. 465–476, 2017